Irregular Geometry Based Sectored FFR Scheme for ICI Mitigation in Multicellular Networks

Rahat Ullah, Hanif Ullah, Zubair Khalid, and Hashim Safdar
Department of Electrical Engineering, FUUAST, Islamabad 4400, Pakistan
Email: {rahatz, hanifuet, engr.zktanoli, hashimsafdar}@gmail.com

Abstract—Future Cellular Systems are aiming aggressive frequency reuse in response to the exponential increase in the data traffic demand. The system capacity boosted accordingly, however, at the expense of increased Inter Cell Interference (ICI). Fractional Frequency Reuse (FFR) is an effective ICI mitigation approach, however, mostly analyzed with regular geometry model in literature. In this paper, Irregular Geometry based Sectored-FFR (IGS-FFR) scheme is proposed for ICI mitigation in the realistic irregular geometry cellular networks. The proposed scheme realize full frequency utilization by dynamic spectrum partition while considering heterogeneous traffic demand. Moreover, the performance of high order sectoring in the cell edge region is investigated. It is shown that the proposed IGS-FFR scheme outperform the existing approaches in terms of achievable throughput, average sum rate and user satisfaction while considering full traffic load.

Index Terms—ICI, Sectored-FFR, irregular geometry model, heterogeneous traffic, dynamic spectrum, user satisfaction

I. Introduction

Next generation cellular systems are targeting aggressive frequency reuse due to the scarcity of frequency spectrum, to meet the ever increasing capacity demand for the mobile broadband applications and services [1]. Such frequent frequency reuse increase the spatial spectrum efficiency and the network capacity, however, at the expense of increased ICI [2]. Therefore, ICI is one of the prominent limiting factors in performance degradation which affect the users' ability to achieve the desire quality-of-service (QoS) [3]. Furthermore, the ICI problem is more severe at the cell edges, if the spectrum management is not carefully considered [4].

Due to the above mentioned challenge, interference mitigation is the primary interest of both the academic and industry communities. To enhance the performance of the cellular network, FFR is an effective ICIC approach [5]. The basic mechanism of FFR corresponds to the partitioning of the cell coverage area in spatial sub-regions. Moreover, the spectrum bands are then allocated to each sub-region in way that avoid the ICI [6]. The main objective of FFR is to improve the SINR and system throughput by avoiding the ICI [7].

Manuscript received May 13, 2020; revised September 23, 2020.
Corresponding author email: rahatz@gmail.com.
doi:10.12720/jcm.15.11.796-807

Network geometry or topology considered for any ICI mitigation scheme plays an important role in terms of performance analysis. FFR is attractive due to its low complexity and significant coverage improvement for cell edge users [8]. However, in literature FFR has been analyzed mostly for the perfect cellular geometry Hexagonal Grid Model (HGM) [9], while no practical deployment has this degree of symmetry [10]. In realistic deployment, where the cellular layout is irregular, not only propagation conditions vary significantly from cell to cell but also azimuths are not aligned and hence, cells receive very different amounts of ICI [11]. As a consequence, cell edges are very different in terms of size and interference levels. Therefore, the performance of traditional FFR schemes are poor in the irregular geometry cellular deployment [12].

These considerations have triggered the research and FFR has been included with irregular geometry cellular networks [13], [14]. However, most of the previous work which includes FFR into irregular geometry model only accounts for simplistic FFR with only two regions (cell-center and cell-edge) and the cell sectoring has not taken into account. Moreover, dynamic spectrum partitioning configuration need to be adopted in the FFR when applied to the irregular geometry cellular network [15]. The dynamic spectrum allocation will enable the system bandwidth to be partitioned in accordance with the network variations and diverse traffic demands [16]–[18].

In this paper, IGS-FFR scheme is proposed as an interference mitigation scheme for the irregular geometry based OFDMA multi-cellular network. Since the irregular geometry cells are considered, cell-partition and sectoring results in the sub-sub regions of the different coverage area and hence different number of users. Cell sectoring is executed with three different angles and the resultant schemes are called IGS-FFR3 (120^0 Sectoring), IGS-FFR4 (90^0 Sectoring) and IGS-FFR6 (60^0 Sectoring). Moreover, heterogeneous traffic demand is considered from each user. Therefore, each sub-region of the cell is having different resource requirement. Applying regular resource partition of the traditional FFR schemes leads to the underutilization of resources and hence degraded performance. In the proposed scheme each cell of the network autonomously decides the spectrum partition according to the requirement of each sub-region of the cell. Moreover, the ICI is avoided by maintaining the orthogonality in the cell-edge sub-band allocation.

The rest of the paper is organized as, System Model is presented in section II, section III gives the problem formulation, section IV presents the development of the proposed IGS-FFR scheme, performance evaluation is done in section V, whereas section VI concludes the paper.

II. System Model

A. Network Topology

In the network topology, OFMDA based multi-cellular network is considered where the BSs are operating in the downlink at a fixed transmits power P^t. To capture the realistic BSs deployment scenario, we assume that the BSs are spatially distributed according to Hard Core Point Process (HCPP) Φ in the Euclidean plane $\mathbb{R}^2$[19]. Furthermore, we assume that the users are randomly distributed in the coverage area and each user is served by its nearest BS in Φ or equivalently, the users are served by the BS that provides the maximum average received signal.

Let X represent a set of points (BSs) on the plane Euclidean plane ($\mathbb{R}^2$). For each given BS x the Voronoi cell $C(x)$ is the set of of all the points that are closer to x than any other point of Φ. Mathematically, Voronoi cell $C(x)$ of x is given by

$$C(x) = \{y \in \mathbb{R}^2 : |y - x| \leq |y - X^i|, \forall X^i \in \Phi\} \quad (1)$$

The Voronoi tessellations characterize the cell boundaries or a BS coverage area [20]. The resultant network layout is shown in Fig. 1, where the inverted triangles show the BSs positions and users' distribution is represented with circular dots.

Moreover, we assume that a user can register with only one BS, hence, getting network access by more than one BS is denied by the system operation. The full buffer model is assumed for the user traffic demand. Specifically, each user minimum data traffic demands are randomly generated within a certain range of data rate values. Therefore, during the simulation there are always data to be transmitted by the fixed number of users in the network.

B. Channel Model

To perfectly analyze the performance of the proposed network topology, it is important to accurately model the effect of the radio propagation channel on the received signal. For a BS i operating in the downlink, the received power on the sub-carrier $k \in K$ by user n can be calculated as

$$P^r_{n,k} = P^t_{n,k} G^i_{n,k} \quad (2)$$

where $P^t_{n,k}$ is the power transmitted by BS on sub-carrier k whereas, $G^i_{n,k}$is the channel gain of the BS i on the sub-carrier k for user n. The channel gain $G^i_{n,k}$ can be mathematically expressed as

$$G^i_{n,k} = |H^i_{n,k}|^2 (10)^{\frac{-PL(D^i_n) * X_\sigma}{10}} \quad (3)$$

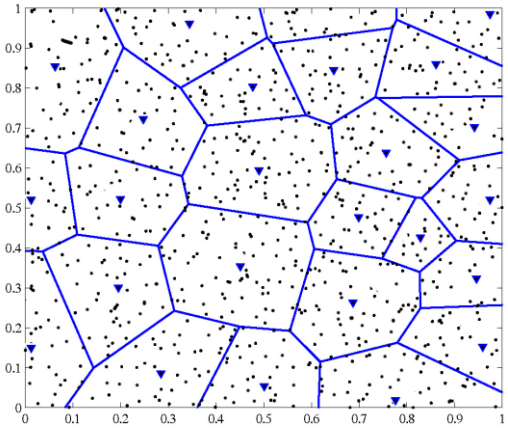

Fig. 1. Voronoi tessellation based network topology

where, $H^i_{n,k}$ represent the small scale fading gain. $PL(D^i_n)$ is the large scale path loss of the distance D^i_n between BS i and user n. Moreover, X_σ represent the log-normal shadowing with the subscript σ which is the value of standard deviation. The small scale channel fading gain between BS and user n on sub-carrier k ($H^i_{n,k}$) is a random variable and follows the Raleigh distribution with unit mean.

C. Path loss Model

The path loss $PL(D^i_n)$ depends on the network topology defined by the locations of the BS and the users. Let the location of BS with index $i \in \Phi$ is represented by $\{X^i \in \mathbb{R}^2\}$ and $\{X^n \in \mathbb{R}^2\}$ represent the location of a user n in the two dimensional space of the network area, then the distance D^i_n can be calculated as

$$D^i_n = \|X^i - X^n\| \quad (4)$$

Note that when considering a random user location in the network, the BS-to-user distance D^i_n becomes another random variable. Based on 3GPP recommendation [21], the path loss $PL(D^i_n)$ can be calculated as;

$$PL(D^i_n) = Prob(D^i_n)^{LOS} * PL(D^i_n)^{LOS} + Prob(D^i_n)^{NLOS} * PL(D^i_n)^{NLOS} \quad (5)$$

where,

$$PL(D^i_n)^{LOS} = 103.4 + 24.2\, log_{10}(D^i_n) \quad (6)$$

$$PL(D^i_n)^{NLOS} = 131.1 + 37.6\, log_{10}(D^i_n) \quad (7)$$

$$Prob(D^i_n)^{LOS} = min\left(\frac{0.018}{D^i_n}, 1\right) * \left(1 - exp\left(-\frac{D^i_n}{0.063}\right)\right) + exp\left(-\frac{D^i_n}{0.063}\right) \quad (8)$$

$$Prob(D^i_n)^{NLOS} = 1 - Prob(D^i_n)^{LOS} \quad (9)$$

In the above equations, D^i_n represents the distance between user n and the base station in the unit of meter (m).

D. The Interference Model

The ICI within the reference cell occurs due to the same spectral utilization in the adjacent cells. In the

multicellular network, the power of the interference received by a user n on sub-channel k can be calculated as

$$I_{n,k} = \sum_{j \in \Phi \setminus i} P_{n,k}^{j} \, G_{n,k}^{j} \tag{10}$$

where Φ represents all transmitting BSs in the $\mathbb{R}^2$. $P_{n,k}^{j}$ and $G_{n,k}^{j}$ are the transmit power and channel gain respectively from the Interferers BSs. By having information about the received signal power and interference signal power, signal quality received by user n can modelled in terms of $SINR$. The downlink received $SINR$ of a user n on sub-carrier k can be calculated for a serving BS i as

$$SINR_{n,k} = \frac{P_{n,k}^{i} G_{n,k}^{i}}{N_o \Delta f + I_{n,k}} \tag{11}$$

N_o is the power spectral density of the additive white Gaussian noise (AWGN) . Obviously, the $SINR$ value of a user depends on the interference signal power. The high interference power received by a user would result in low $SINR$ values. Eventually, with the degraded $SINR$ values would result in, low user throughput and hence low network performance. Therefore, a proper spectrum management needs to be considered for the inter cell interference mitigation in the multicellular environment.

III. Problem Formulation

In this section formulation of the proposed IGS-FFR scheme is presented. This formulation is based on the channel model equation presented in the previous section, where the mathematical expression for the interference signal is derived in equation (11). Therefore, the $SINR$ of a user n on sub-channel k can be computed as in equations (11) given that the intended signal strength for the user n is expressed in equations (2). Note that K (where $k \in K$) is the total number of sub-carriers in the available system bandwidth (B^T) for N number of total users (where $n \in N$).

Therefore, the spectral efficiency ($SE_{n,k}$) of a user n can be calculated in the unit of bit per second (bps)

$$SE_{n,k} = log_2\left(1 + SINR_{n,k}\right) \tag{12}$$

Using the Shannon's theorem, we can find the throughput $R_{n,k}$ of a user n on sub-carrier k as

$$R_{n,k} = \Delta f \, SE_{n,k} \tag{13}$$

where Δf is the sub-carriers spacing. Therefore, when a user is assigned with more than one sub-carriers, the achievable throughput R_n of a user can be calculated as an aggregate of the $SE_{n,k}$ on all sub-carriers that are assigned to the user n.

$$R_n = B_n^a \sum_{k=1}^{K_n} S_{n,k} \tag{14}$$

Where B_n^a is the bandwidth allocated to user n and $K_n = (B_n^a/\Delta f)$ is the number of sub-carriers in B_n^a. Equation (14) can also be written as

$$R_n = \Delta f \sum_{k=1}^{K} x_{n,k}.S_{n,k} \tag{15}$$

where $x_{n,k}$ be the sub-carrier allocation indicator,

$$x_{n,k} = \begin{cases} 1, & k \; is \; allocated \; to \; user \; n \\ 0, & otherwise \end{cases} \tag{16}$$

The overall throughput of a serving cell i can be expressed as

$$R_N^i = \sum_{n=1}^{N} R_n \tag{17}$$

The mathematical expression shown in equation (14) clearly shows that more is the number sub-carrier allocated to a user, higher will be the achievable rate of that user. However, the rate depends on the spectral efficiency, which is the function of received SINR. Therefore, the low user SINR that is attributed by interference existence would result in low spectral efficiency and will eventually degrade the user achievable throughput. In the multicellular system interference is more rigorous remarkably at the cell edges.

In this research work, FFR based spectrum management is adopted to avoid ICI. The Cell coverage area is divided into cell-center and cell-edge regions based on threshold SINR. Moreover, to fully utilize the available spectrum resources, the cell edge region is further divided into a number of sectors. Interference avoidance is achieved through an orthogonal spectrum assignment at cell-edge region. Based on this requirement, a self-organized spectrum partitioning configuration is propose, which enables the total system bandwidth to be partitioned into flexible orthogonal sub-bands to support the dynamics of the spectrum requirement of each sub-region of a cell.

Therefore, the problem of dynamic spectrum partition in the proposed IGS-FFR scheme can be formulated as the total achievable throughput maximization problem. Mathematically the resource allocation problem can be expressed as

$$\underset{\{B^T\}}{max} \left(\sum_{n=1}^{N} \sum_{k=1}^{K} x_{n,k} \, R_{n,k} \right) \tag{18}$$

$$subject \; to \begin{cases} x_{n,k} = \{0,1\} & (19) \\ \sum_{n=1}^{N} x_{n,k} = 1, for \; \forall \, n & (20) \end{cases}$$

where B^T is total available system bandwidth. The objective of the resource allocation problem is to maximize the overall throughput of the system while allocating the total bandwidth. The constraint in equation (19) indicates the problem is binary integer type and equation (20) indicates that each sub-carrier can be allocated to only one user in the cell.

IV. Development of IGS-FFR scheme

This section presents the proposed IGS-FFR scheme for irregular geometry OFDMA multi-cellular network.

To accomplish the objective of overall system throughput maximization, the IGS-FFR scheme split the cell coverage area into a number of sub-regions. The total available spectrum resources are allocated to each sub-region based on the bandwidth requirement. Moreover, ICI is greatly avoided in the cell edge region by allocating the orthogonal sub-band to the neighboring sector in the multicellular environment. The overall flow chart of the proposed scheme is presented in Fig. 2.

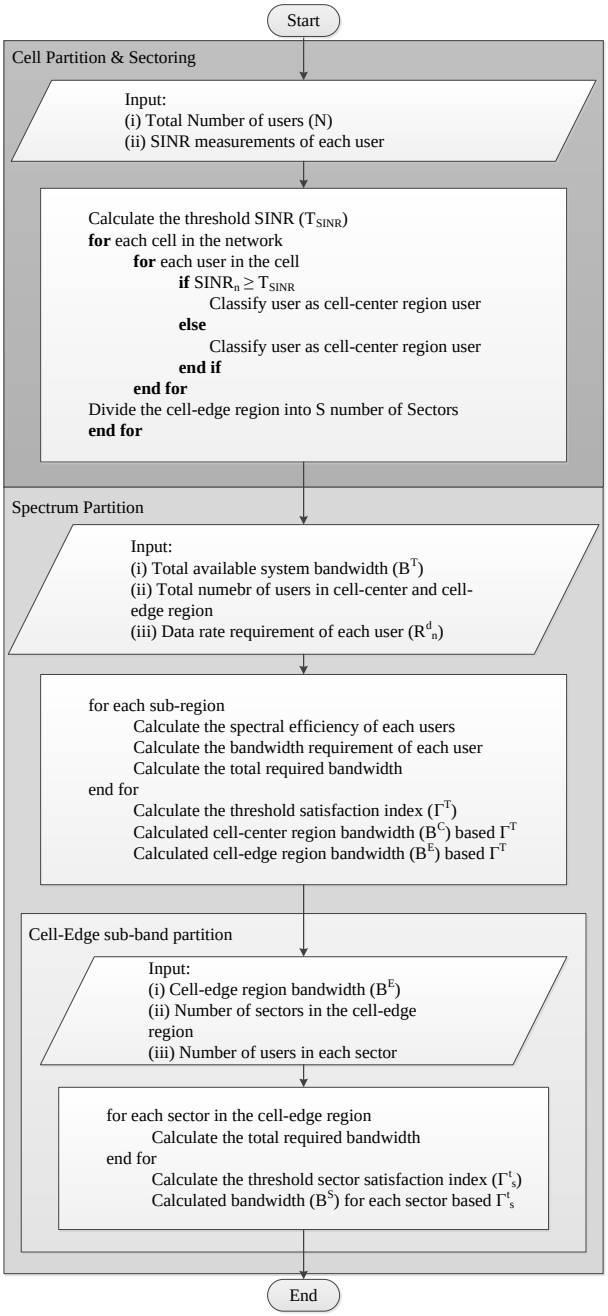

Fig. 2. The overall flow of the IGS-FFR algorithm

As mentioned in the flow chart, the proposed IGS-FFR scheme is composed of two main sections. The first section is 'cell-partition and sectoring' section, where each cell of the network is divided into cell-center region and cell-edge region. The users are classified as cell-center or cell-edge user based on the SINR measurements. Threshold SINR (T_{SINR}) is independently calculated at each cell of the network to decide the cell-partition. Moreover, the cell-edge region is further divided into a number of sectors. Since, the cells are irregular geometry, the resultant sub-regions are also irregular both in terms of geometry and traffic load. Hence, the spectrum resources are needed to be dynamically allocated according to the demand of each sub-region.

The Second section is the 'spectrum partition', where the total available bandwidth is dynamically partition for each sub-region, based on the spectrum demand or traffic load. Spectrum partition is autonomously performed by each BS of the network in the self-organization manner. Spectrum partition is done in two phases. Initially, the total spectrum is divided into cell-center and cell-edge band while considering the spectrum requirement of both regions by calculating the threshold satisfaction index. Consequently, the cell-edge sub-band is partitioned into sector's sub-bands based on the spectrum requirement of each sector.

A. Cell Partition and Sectoring

Cell partition is one the vital design considerations in the FFR to classify cell-center and cell-edge users. Since, each cell is having random coverage area represented by Voronoi tessellation. The classical distance based cell-partition is not feasible with such geometry. Moreover, the cell-center and cell-edge users do not have same geographic interpretation. Therefore, in this work, the average received $SINR$ is taken as a threshold (T_S) to classify the cell-center and cell-edge users, as $SINR$ is the best measure of the distance between the user and the serving BS. The BS decides the users N based on T_S, users with the received $SINR$ greater than T_S are defined as cell-center users N^C, whereas, users with average $SINR$ less that T_S are defined as cell-edge users N^E.

In addition to the cell partition, the cell-edge region is further divided into S number of sectors in the proposed IGS-FFR scheme. Therefore, the cell-edge users N^E is the sum of the users at each sector N^s, that is

$$N^E = \sum_{s=1}^{S} N^s \tag{21}$$

where $S = \{3,4,6\}$, $S = 3$ corresponds to 120^o sectoring of the cell-edge region and the resultant scheme is IGS-FFR3 scheme. S=4 corresponds 90^o sectoring of the cell-edge region and the resultant scheme is IGS-FFR4 scheme. Whereas, S=6 corresponds to 60^o sectoring of the cell-edge region and the resultant scheme is IGS-FFR6 scheme. We assume the interference from the first tier of the neighbor cells (adjacent cells), therefore, for an irregular cell with seven sides, the network size is a cluster of eight cells. The resultant network for the IGS-FFR3, IGS-FFR4 and IGS-FFR6 are shown in the Fig. 3, Fig. 4 and Fig. 5 respectively.

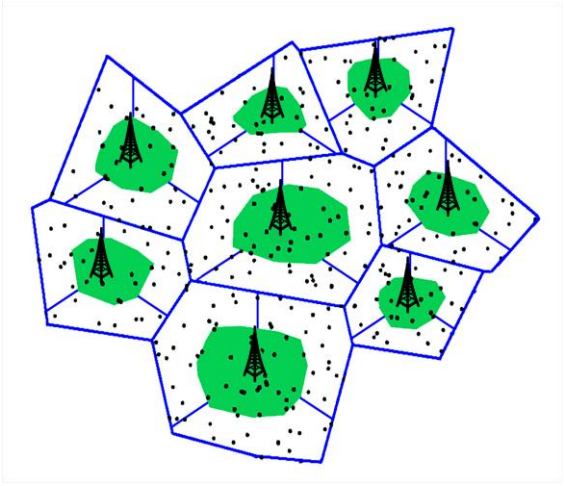

Fig. 3. Irregular geometry based multi-cellular network for the IGS-FFR3

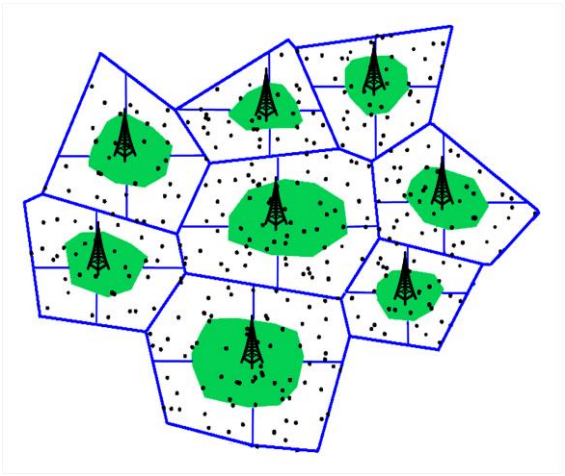

Fig. 4. Irregular geometry based multi-cellular network for the IGS-FFR4

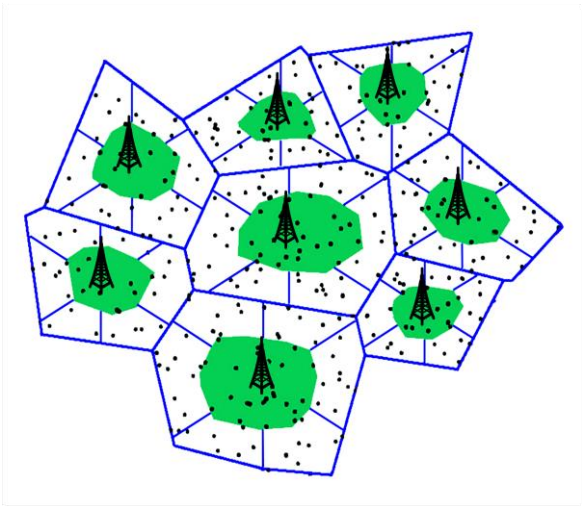

Fig. 5. Irregular geometry based multi-cellular network for the IGS-FFR6

B. Spectrum Partition

The total available spectrum is partitioned into sub-bands to be allocated to each sub-region of the cell. The changes in the network parameters, particularly the traffic load and spectrum requirement are autonomously observed and the spectrum partition is performed accordingly. A decentralized approach has been advised, where the spectrum partition is autonomously performed at each BS taking as input some limited data from the environment. The spectrum partition flow chart is shown in the Fig. 6.

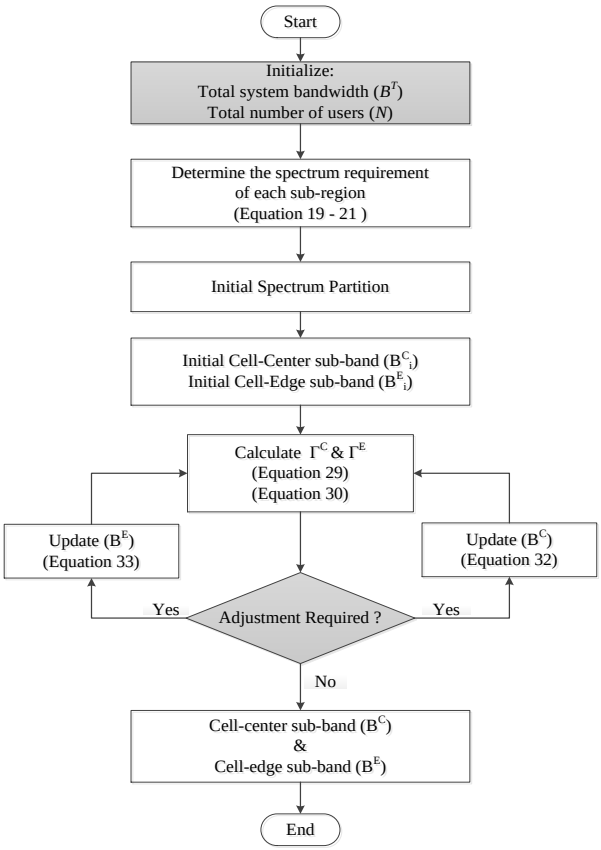

Fig. 6. The IGS-FFR spectrum partition (cell-center and cell-edge band) flow chart

C. Estimation of the Spectrum Requirement

To estimate the required spectrum for each sub-region of a cell, first the number of sub-carriers required by each user of the corresponding sub-region must be calculated. The estimated bandwidth requirement B_{req}^n of a user n to meet the traffic demand R_d^n can be calculated as

$$B_{req}^n = \left(\frac{R_d^n}{SE_n}\right) \tag{22}$$

where SE_n is the spectral efficiency of a user n, which is the function of the received SINR as shown in equation (12). The bandwidth required B_{req}^n by a user n is proportional to its demand rate and inversely proportional to the spectral efficiency. Therefore, spectrum allocation is based on the channel quality information such as spectral efficiency marks the proposed IGS-FFR scheme to exploit the multiuser diversity in OFDMA operation.

The estimated number of sub-carriers required by a user to fulfill its traffic demand can be calculated as

$$K_{req}^n = \left\lceil \frac{B_{req}^n}{\Delta f} \right\rceil \tag{23}$$

where Δf is the size of each sub-carrier in the network. Equation (23) shows that the number of requested sub-carrier can be calculated using the ceiling function. For example, if the division results in 1.5, it will be converted to 2 as the network is not able to allocate half of the sub-carrier.

Once the bandwidth requirement of each user B_{req}^{n} in the sub-region is known, then the bandwidth required by that particular sub-region can be calculated. Since the total number of user N is the sum of the user at each sub-region.

$$N = N^C + N^E = N^C + \sum_{s=1}^{S} N^s \tag{24}$$

where N^C is the total number of user at cell-center region, N^E is the total number of users at the cell-edge region and N^S is the number of users at sector S of the cell-edge region. Therefore, the bandwidth required by cell-center region B_{req}^{c}, cell edge region B_{req}^{e} and cell-sector region B_{req}^{s} can be calculated as

$$B_{req}^{c} = \sum_{n=1}^{N^C} B_{req}^{n} \ , \qquad (n \in N^C) \tag{25}$$

$$B_{req}^{e} = \sum_{n=1}^{N^E} B_{req}^{n}, \qquad (n \in N^E) \tag{26}$$

$$B_{req}^{s} = \sum_{n=1}^{N^S} B_{req}^{n}, \qquad (n \in N^E) \tag{27}$$

D. Cell-Center and Cell-Edge Sub-bands

Let B^T is the total available bandwidth to be utilized in the cell-center and cell-edge region. The $B^T$is innitially the partition into cell-center sub-band B_i^C and cell-edge sub-band B_i^E based on the threshold $SINR$ (T_S). However, these sub-bands are adjusted dynamically according to the traffic load. The average received $SINR$ is selected as a threshold.

$$B^T = B_i^C + B_i^E \tag{28}$$

The bandwidth resources are limited in each region of the cell. We assume that the bandwidth allocated to each sub-region is less than the required bandwidth. In order to find that how close is the allocated bandwidth to the required bandwidth, we calculate the satisfaction index of each sub-region of the cell. The satisfaction index of a sub-region is the ratio of the allocated bandwidth to the required bandwidth. Therefore, the cell-center region satisfaction index Γ^C and cell-edge region satisfaction index Γ^E ar are given by the following equations respectively.

$$\Gamma^C = \frac{B_i^C}{B_{req}^{c}} \tag{29}$$

$$\Gamma^E = \frac{B_i^E}{B_{req}^{e}} \tag{30}$$

The satisfaction index computed by equation (29) and equation (30) will lie in (0,1) range. In order to adjust the allocated bandwidth according to the traffic demand, we introduce the threshold satisfaction index Γ^T. The threshold satisfaction index Γ^T is average of the satisfaction index for cell-center region $\Gamma^C$and cell-edge region Γ^E , is given by

$$\Gamma^T = \frac{\Gamma^C + \Gamma^E}{2} \tag{31}$$

Consequently, the bandwidth allocated to cell-center region B^C and the bandwidth allocated to cell-edge region B^E are updated according to the following two equations respectively.

$$B^C = \Gamma^T\left(B_{req}^{c}\right) \tag{32}$$

$$B^E = \Gamma^T\left(B_{req}^{e}\right) \tag{33}$$

The satisfaction index for cell-center and cell-edge region (Γ^C, Γ^E) would results in equal values when computed based the updated sub-bands B^C and B^E. This means the initial spectrum partition is adjusted according to the traffic demand of each sub-region. The spectrum sub-band B^C is allocated directly to the cell-center region users, whereas the sub-band B^E is further partitioned into sub-bands for each sector the cell-edge region users. The number of sub-carriers in the cell-center sub-bands B^C can be calculated by using the following equation

$$K^C = \left\lfloor \frac{B^C}{\Delta f} \right\rfloor \tag{34}$$

Note the floor is selected to estimate the number of sub-carrier in the sub-band to ensure that the allocated sub-carriers may not exceed the total number of sub-carriers of the system.

E. Cell-Edge Sub-band Partition

In order to fully utilize the cell-edge sub-band B^E in each cell of the network, the cell-edge region has been divided into S numbers of sectors. The resultant sectors are having random coverage region and different number of users. Considering the traffic demand of each sector, the load distribution is uneven. Therefore, the proposed scheme allocates the cell-edge band to satisfy the load condition of each sector. The bandwidth requirement of each sector can be determine using equation (27). Moreover, the orthogonality of the neighboring cell-edge band is upheld in order to avoid the inter cell interference. Therefore, the cell-edge sub-band B^E is divided into $S + 1$ equal sub-bands ($B^1, B^2, \ldots . B^S, B^o$).

$$B^E = B^1 + B^2 +, \ldots . B^s + B^o \tag{35}$$

In case of IGS-FFR3,

$$B^E = B^1 + B^2 + B^3 + B^o \tag{36}$$

Sub-bands $B^1, B^2, \ldots . B^S$ are dedicated for sector-1, sector-2,….sector-S respectively. Moreover, we assume that these dedicated sub-bands ($B^1, B^2, \ldots . B^S$) are less than the required bandwidth of each sector. Whereas, the sub-band B^o is open to all sectors and portion of it can be allocated to each sector based on the traffic demand and load distribution. Let B_s^o represents the portion of the open sub-band B^o to be allocated to sector S. To find B_s^o for each sector S, we define the sector satisfaction index Γ^S which is given by

$$\Gamma^S = \frac{B_a^s}{B_{req}^s} \quad (37)$$

where B_{req}^s is the bandwidth required by sector S (given by equation (27)) to fulfill its traffic demand and B_a^s is the bandwidth allocated to sector S. The B_s^o for each sector is calculated in two steps. Initially, when each sector is allocated with B^S or in other words when $B_a^s = B^S$, and Γ^S computed for each sector would result in different values for each sector, depending upon the bandwidth requirement of each sector. In the first step, the maximum of the satisfaction index Γ^S is selected as a threshold Γ^t and a portion of sub-band $B_{s,i}^o$ is calculated for all sectors. The addition of $B_{s,i}^o$ in the allocated sub-band for each sector would results in equal Γ^S for all sectors. In the second step $B_{s,f}^o$ is calculated for each sector out of the remaining sub-band $B^{o\prime}$ based on to the demand of each sector. The threshold satisfaction index is given by

$$\Gamma_s^t = \max(\Gamma^1, \Gamma^2 \ldots . \Gamma^S) \quad (38)$$

Based on Γ^t, $B_{s,i}^o$ can be calculated for each sector as

$$B_{s,i}^o = \Gamma_s^t\left(B_{req}^s\right) - B^s \quad (39)$$

Equation (39) determines the initial amount of sub-band $B_{s,i}^o$ to be allocated to each sector out of open sub-band Bo. After the initial sub-band allocation $B_{s,i}^o$, the remainder of the open sub-band is calculated as

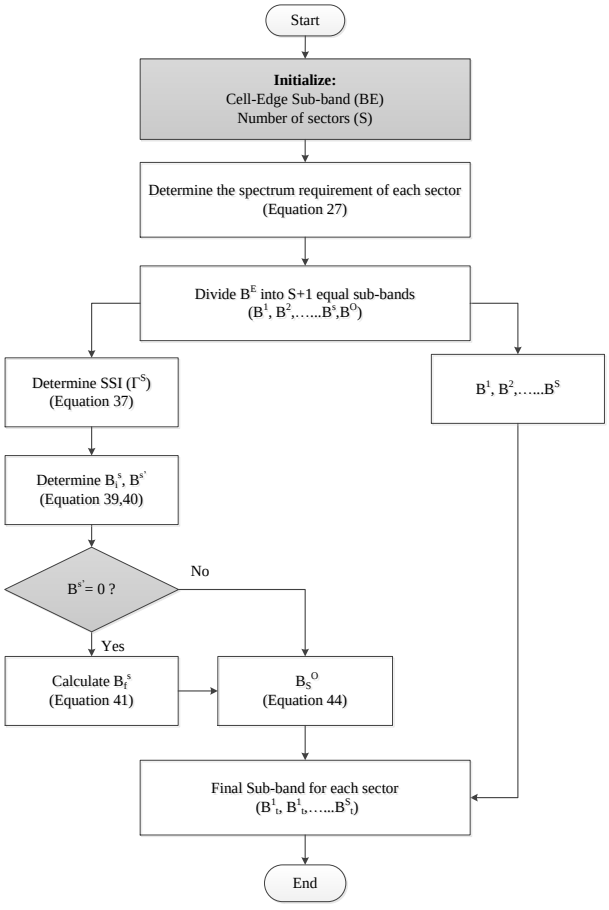

Fig. 7. The IGS-FFR cell-edge band partition flow chart

$$B^{o\prime} = B^o - \sum_{s=1}^{S} B_{s,i}^o \quad (40)$$

If $B^{o\prime} \neq 0$, then the final sub-band $B_{s,f}^o$ is calculated as

$$B_{s,f}^o = \left(\frac{B_i^s}{B_t^e}\right)\left(B^{o\prime}\right) \quad (41)$$

where, B_i^s is the initial sub-band allocated to sector S and B_t^e is the total amount of bandwidth allocated so far to the cell-edge region, B_i^s and B_t^e are given by following two expressions respectively,

$$B_i^s = B^S + B_{s,i}^o \quad (42)$$

And

$$B_t^e = \sum_{s=1}^{S} B_i^s \quad (43)$$

Therefore, the amount of sub-band B_s^o out of the open sub-band B^o is given by

$$B_s^o = B_{s,i}^o + B_{s,f}^o \quad (44)$$

Finally the total bandwidth B_t^S to be allocated at a sector S can be calculated as,

$$B_t^S = B^S + B_s^o \quad (45)$$

where B^S is equal for all sectors, however B_s^o is calculated based on the sector threshold satisfaction index. The flow chart of the spectrum partition is shown in Fig. 7. The number of sub-carriers K^S in the each sector sub-band BS can be computed as

$$K^S = \left\lfloor \frac{B_t^S}{\Delta f} \right\rfloor \quad (46)$$

The floor function in equation (46) ensures that number of allocated sub-carriers may not exceed the total number of available sub-carriers in the total spectrum.

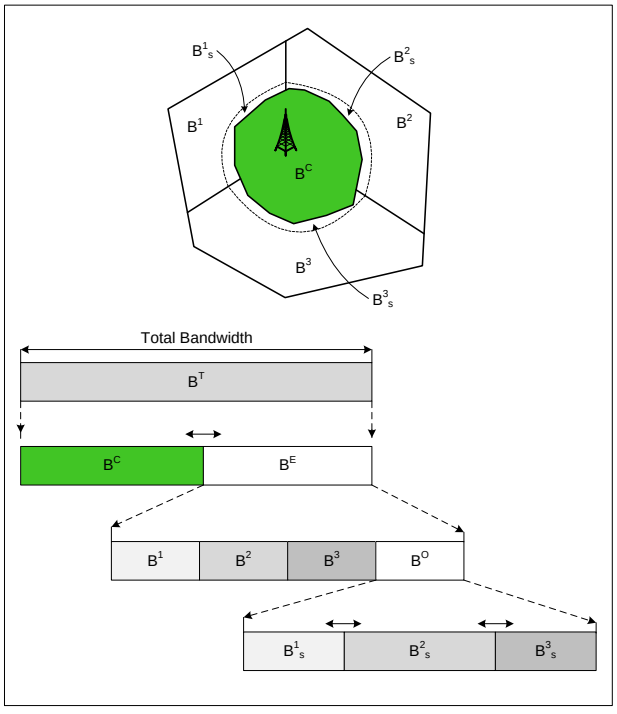

Fig. 8. Illustration of the spectrum partition for IGS-FFR3 scheme.

To maintain the orthogonality in the cell-edge sub-band of the neighboring cell, B^s is specified for outer region of a sector, whereas B_s^o is specified for the inner region of a sector near to cell-center region. However, there is no specific boundary for a sector outer and inner region as the sub-band B_s^o is dynamic and it changes according to load condition and traffic demand for each sector. The spectrum partition and allocation for IGS-FFR3 scheme is elaborated in Fig. 8. In the proposed scheme, the sub-band for each sub-region are calculated according to the traffic demand of that sub-region. Then the sub-carriers of each sub-band are allocated randomly to the users of that particular sub-region. The random selection aims at averaging the quality of the subcarriers while it has the advantage that it needs no channel state information.

V. Performance Analysis of the Proposed Scheme

This section presents the performance analysis of the proposed IGS-FFR scheme for the irregular geometry cellular network along with the simulation setup. The performance analysis is done in two phases. First, the IGS-FFR3 scheme is compared with the number of reference schemes available in the literature. Then, to analyze the performance of high order sectoring in the irregular geometry multi-cellular network, the IGS-FFR3 scheme is compared with IGS-FFR4 and IGS-FFR6 scheme.

A. Simulation Setup

In the network model, a cluster of eight irregular geometry cells are considered. The BSs are positioned based on HCPP. Therefore, unlike the regular or hexagonal grid, the inter site distance is random. The inter cell distance is generated randomly in the range of 600 to 1000 meters. This means that the closest possible BS that can cause the ICI is 600 meters of the serving BS. Moreover, each BS is serving a fixed number of user N=100, randomly distributed in the coverage region of each cell. The heterogeneous traffic load is considered which means that users are having diverse traffic. User demand is generated using the random distribution function in the range of $(30kbps, R_d^{max})$. The lower bound of the traffic is set to $30kbps$ in order to meet the conventional web-browsing demand. The upper limit is set as $R_d^{max} \in \{100,200, \ldots \ldots \ldots 1000\}$kbps.

The following expression can be used to convert the specific traffic condition of the network load.

$$Load = \left(\frac{N * (R^{mean})}{N * R_{max}^{mean}}\right) \quad (47)$$

The user traffic demand is generated randomly, therefore the load calculation considers the current mean rang $R^{mean} = (30 + R_{max})/2$ kbps and the maximum mean range $R_{max}^{mean} = (30 + 1000)/2$ kbps. To maintain the user load distribution during the simulation, the user mobility is not considered. Moreover, the general parameters used in simulation are listed in the Table I.

The achievable throughput is computed based on the Shannon's theorem, which leads to the upper bound of the user throughput in bits per second. Expression for the cell throughput R total cell is given as follows

$$R_{total}^{cell} = R_{center} + \sum_{s=1}^{S} R_s \quad (48)$$

where R_{center} represents the achievable rate or throughput of the cell center region, which can be calculated as

$$R_{center} = B^C \sum_{n=1}^{N^C} log_2(1 + SINR_n) \quad (49)$$

where, N^C is the number of users in the cell-center region, and B^C is bandwidth allocated to cell-center region. In terms of sub-carriers allocation the above expression can be written as

$$R_{center} = \Delta f \sum_{n=1}^{N^C} \sum_{k=1}^{K^C} log_2\left(1 + \left(SINR_{n,k}\right)\right) \quad (50)$$

where K^C is the maximum number of sub-carriers in the cell center region and can be found by equation (34). Similarly the R_s equation (48) represent the achievable rate of the sector S of the cell-edge region and can be computed as follows

$$R_s = B_t^s \sum_{n=1}^{N^S} log_2(1 + SINR_n) \quad (51)$$

where, N^S is the number of users in the cell-center region, and B_t^s is bandwidth allocated to sector S of the cell-edge region.

The total number of sub-carriers in sub-band B_t^s is K^S and can by found using equation (46). Therefore, in terms of sub-carriers allocation equation (51) can be written as

$$R_s = \Delta f \sum_{n=1}^{N^S} \sum_{k=1}^{K^S} log_2\left(1 + \left(SINR_{n,k}\right)\right) \quad (52)$$

TABLE I. SIMULATION PARAMETERS

Network Parameter	**Values**
Cellular layout	HCPP based irregular geometry (Voronoi)
Network Size	8 Irregular Cells
Number of users per cell	100
Inter cell distance	Random
Carrier Frequency	2GHz
System Bandwidth	10MHz
No of sub-carriers	600
Sub-carrier spacing	15KHz
BS transmits power	46dBm
White noise power density	-174dBm/Hz
Shadowing standard deviation	8dB
Multipath fading	Rayleigh fading

B. Performance Analysis of IGS-FFR3 Scheme

In order to validate the performance of the proposed IGS-FFR3 schemes, obtained results are compared with the number of reference schemes available in the literature, such as Reuse-1, Strict-FFR, and FFR-3 schemes when applied to irregular geometry multi-cellular system. Specifically, to make the analysis more significant and meaningful, the proposed IGS-FFR3 scheme is compared with Reuse-1 scheme, which is a generalized scheme and utilize total system bandwidth at every cell of the network. The proposed scheme is also compared with Strict-FFR scheme. Moreover, the proposed IGS-FFR3 scheme is compared with traditional FFR-3 scheme. FFR-3 scheme also called sectored-FFR scheme.

- *CDF of the Achievable Throughput for IGS-FFR3*

Fig. 9, shows the Cumulative Density Function (CDF) of users' throughput. The results shows that the proposed IGS-FFR3 scheme outperforms all the basic frequency allocation schemes when applied to the irregular geometry cellular network. Compared to Reuse-1, which allocated all the spectrum resources at every cell of the network, there is 89.6 % increase in the users' throughput for the proposed IGS-FFR3 scheme. The propose scheme also utilize full system bandwidth at every cell of the network, however, the interference is avoided due to the orthogonal sub-bands in the cell-edge region and hence, significant improvement in the users' throughput.

Similarly, compared to the Strict-FFR scheme, there is 40.8 % improvement in the users' throughput for the proposed scheme. Strict-FFR also called FFR(1,3) scheme, uses the frequency reuse of one FR-1 at the cell-center region and frequency reuse of three FR-3 at the cell-edge region. Consequently, Strict-FFR scheme utilizes 2/3 of the total spectrum at each cell of the network. Therefore, the proposed scheme which utilizes frequency reuse of FR-1 at every cell of the network outperforms Strict-FFR scheme. Finally, the proposed scheme is compared to the FFR-3 scheme. Similar to the proposed IGS-FFR3 scheme, the FFR-3 scheme also divides the cell into cell-center and cell-edge regions. Moreover, both schemes further partition the cell-edge region in three sectors in order to realize full spectrum reuse. However, the varying traffic load and spectrum requirement due to the irregular layout of the cells, are not adopted by the basic FFR-3 scheme. As a result, the CDF of users' throughput is improved by 18.3 % for the proposed IGS-FFR3 scheme compared to FFR-3 scheme.

- *Average Sum Rate for IGS-FFR3*

The average sum rate of the cell, cell-center and cell-edge region for the proposed IGS-FFR3 scheme is plotted in the Fig. 10 along with the Strict-FFR and FFR-3 schemes. The average sum rate plot also shows that the proposed IGS-FFR3 scheme improves the average sum rate of the cell by 44.8 % compared to the Strict-FFR.

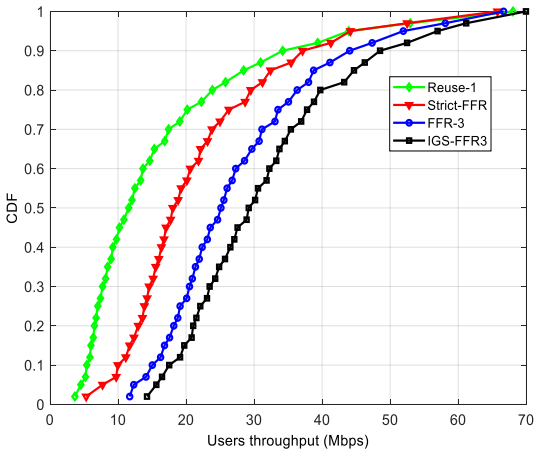

Fig. 9. CDF of the users' throughput

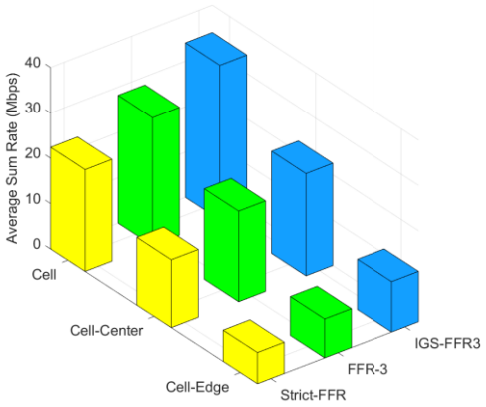

Fig. 10. Average sum rate

Whereas, compare to the basic FFR-3 scheme, the average sum rate of the cell is enhanced by 18 %. The proposed scheme shows 32.6 % and 12.7 % improvement in the cell-center region average sum rate compare to Strict-FFR and FFR-3 schemes respectively. Similarly, the proposed IGS-FFR3 scheme enhances the cell-edge region average sum rate by 62 % and 24 % compared to Strict-FFR and FFR-3 schemes respectively.

- *Achievable Throughput with Respect to Load for IGS-FFR-3*

Fig. 11 shows the results for the cell achievable throughput with respect to load for Reuse-1, Strict-FFR, FFR-3 and IGS-FFR3 schemes. The traffic demand of the users in the cell is translated to load based on equation (47). In the Fig. 11, the value of the load approaches to 1 implies that 100% load of the cell. Results show that the proposed scheme outperforms the Reuse-1 scheme by 68.4 %. Similarly the achievable throughput with respect to the load of the cell for the IGS-FFR3 scheme is enhanced by 38.2 % and 12.3 % compared to Strict-FFR and FFR-3 schemes. This improvement in the system performance in terms of achievable throughput with respect to different load scenario is due to the allocation of the spectrum resource according to the load condition of each sub-region of the cell.

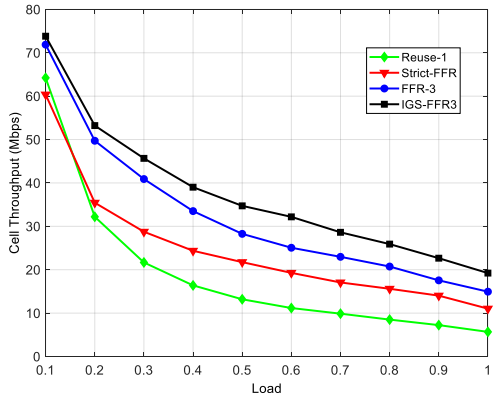

Fig. 11. Cell throughput verses load

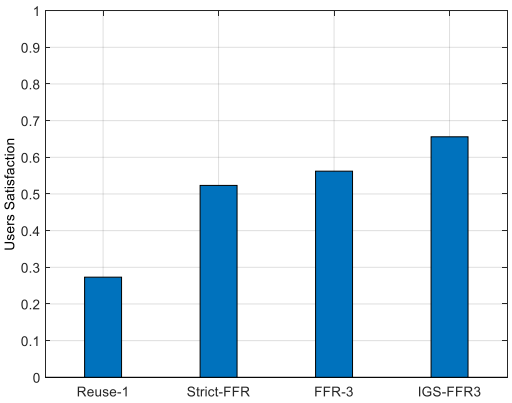

Fig. 12. User satisfaction for different schemes

- *Users' Satisfaction for IGS-FFR3*

User satisfaction is the sum of users throughout divided by the total number of users into maximum user throughput, given by

$$US = \left(\frac{\sum_{n=1}^{N} R_n}{R_{max}.N}\right) \quad (53)$$

User satisfaction shows how closely is the user throughput to the maximum throughput of a user in the cell. It ranges between 0 and 1, when US approaches 1, means that all the users in the cells are experiencing the same throughput. Whereas, US approaches to 0 means that there is a huge variation in the achievable throughput of the users in the cell. Fig. 12 shows the users' satisfaction for the Reuse-1, Strict-FFR, FFR-3 and IGS-FFR3 scheme.

The proposed IGS-FFR3 scheme outperforms the Reuse-1 scheme by 112.5 %, Strict-FFR scheme by 65.8 % and FFR-3 by 38.7 % respectively. The throughput of the cell-center region users are normally very high compared to the cell-edge user of a cell. This is because the cell-edge users are more exposed to interference. Therefore, there is a huge gap between the user throughput and the throughput of a user with maximum throughput in the cell. The proposed scheme enhances the cell-edge performance by allocating the orthogonal sub-bands to avoid the ICI and according to the requirement of the sub-region.

C. Performance Analysis IGS-FFR4 and IGS-FFR6 Schemes

This section analyze the effect of higher order sectoring in the irregular geometry based multicellular OFDMA network for the proposed IGS-FFR scheme.

- *CDF of the Achievable Throughput for IGS-FFR4 and IGS-FFR6*

Fig. 13 gives the CDF of the achievable throughput for IGS-FFR3, IGS-FFR4 and IGS-FFR6 schemes. It shows that with increasing the number of sectors in the cell-edge region the CDF of the users' achievable throughput increases. The users' achievable throughput is enhanced by 21% for IGS-FFR4 compare to the IGS-FFR3 scheme. Moreover, there is a 33% improvement in the users' achievable throughput for IGS-FFR6 compare to the IGS-FFR3 scheme. Compare to IGS-FFR4, 12% improvement in the user throughput is achieved with the IGS-FFR6 scheme. These results show that higher order sectoring in the irregular geometry cellular network improve the system performance by utilizing spatial diversity.

- *Average Sum Rate for IGS-FFR4 and IGS-FFR6*

The average sum rate of IGS-FFR4 and IGS-FFR6 is compared with the IGS-FFR3 scheme. Results for the average sum rate of the overall cell, cell-center and cell-edge region are plotted in the Fig. 14. The average sum rate improved by 20% and 32.7% for IGS-FFR4 and IGS-FFR6 respectively, compared to IGS-FFR3. The average sum rate of the cell-edge and cell-center regions is improved by 45% and 20% respectively for the IGS-FFR6 scheme. Similarly, with IGS-FFR4 scheme compared to IGS-FFR3, the average sum rate increased by 24.7% and 11% for the users of cell-edge and cell-center region respectively. These statistics shows that, the system performance in terms of average sum rate improves with increasing number of sectors in the cell-edge region for the proposed IGS-FFR scheme.

- *Achievable Throughput IGS-FFR4 and IGS-FFR6 with Respect to load*

The average throughput of the cell with respect to load in plotted in the Fig. 15. The average throughput of the cell with respect to load increased by 15.5% for IGS-FFR4 as compared to IGS_FFR3 scheme. Similarly, the average throughput of the cell with respect to load increased by 22.4% for IGS-FFR6 compared to IGS_FFR3 scheme. Moreover, comparing the results for IGS-FFR4 and IGS-FFR6 scheme, there is 7% improvement in the cell achievable throughput for the IGS-FFR6 scheme. Therefore, by increasing the number of sectors in the cell-edge region from 3 to 4 results in 15.5%, from 3 to 6 results in 20.4% and from 4 to 6 results in 5% enhancement in the cell achievable throughput with respect to different load conditions.

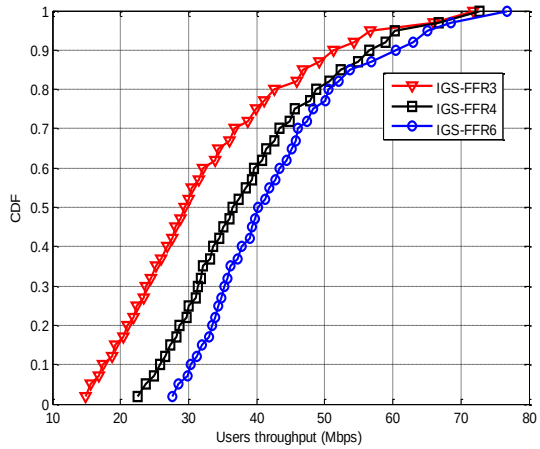

Fig. 13. CDF of the users' throughput for IGS-FFR3, IGS-FFR4 and IGS-FFR6

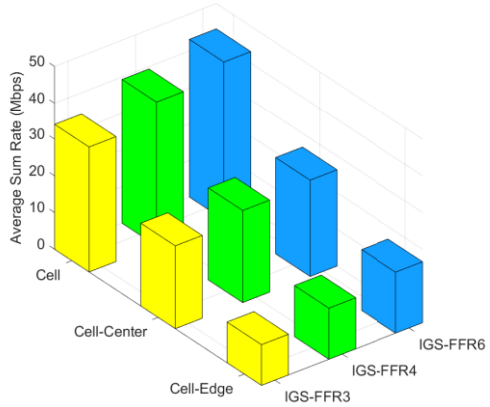

Fig. 14. Average sum rate for IGS-FFR3, IGS-FFR4 and IGS-FFR6

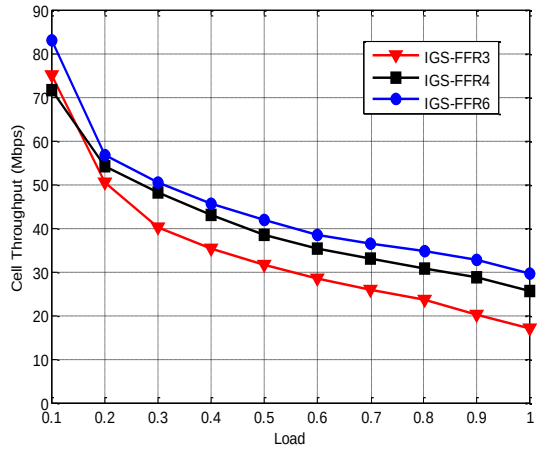

Fig.15. Cell throughput verses load for IGS-FFR3, IGS-FFR4 and IGS-FFR6

VI. Conclusion

In this paper, IGS-FFR scheme is developed as an ICI mitigation scheme for the irregular geometry based OFDMA multicellular network. In order to capture the realistic scenario, irregular geometry based network model is considered. The position of the BSs is abstracted based on PHPP and the users are randomly distributed in the coverage region of each BS. The BSs are operating in the downlink and the coverage region of each cell is represented by a Voronoi shape. In order to overcome the limitations of the basic FFR schemes, when applied to irregular cell geometry networks, the proposed scheme partitioned the cell into cell-center and cell-edge region based on the SINR measurements. Moreover, to fully utilize the total available spectrum resources, the cell-edge region is further divided into a number of sectors.

Since the irregular geometry cells are considered, cell-partition and sectoring results in the sub-regions of different coverage area and hence different number of users. Moreover, heterogeneous traffic demand is considered from each user, therefore, each sub-region of the cell is having different spectrum resource requirement. The IGS-FFR scheme is developed to dynamically decide the spectrum partition according to the requirement of each sub-region of the cell. Moreover, the ICI is avoided by maintaining the orthogonality in the cell-edge sub-band allocation. It is shown that the proposed scheme outperform the existing FFR based ICI mitigations schemes in terms of achievable throughput, average sum rate and user satisfaction while considering full traffic load. Moreover, it is shown that increasing the number of sectors in the cell edge region, improves the system performance.

Conflict of Interest

The authors declare no conflict of interest.

Author Contributions

Dr. Rahat Ullah conducted the research and wrote the paper. Dr. Hanif Ullah and Dr. Zubair Khalid analyzed the data whereas Dr. Hashim Safdar review the final version of the manuscript. All the authors had approved the final version.

References

[1] F. Ali, H. Yigang, G. Shi, Y. Sui, and H. Yuang, "Future generation spectrum standardization for 5G and internet of things," *J. Commun.*, vol. 15, no. 3, pp. 276–282, 2020.

[2] S. U. Abdullahi, J. Liu, and S. A. Mohadeskasaei, "Efficient resource allocation with improved interference mitigation in FFR-aided OFDMA heterogeneous networks," *J. Electron. Sci. Technol.*, vol. 17, no. 1, pp. 73–89, 2019.

[3] F. Qamar, M. H. D. N. Hindia, K. Dimyati, K. A. Noordin, and I. S. Amiri, "Interference management issues for the future 5G network: A review," *Telecommunication Systems*, vol. 71, no. 4, pp. 627–643, 2019.

[4] M. A. Safwat, "Performance evaluation of eICIC scheme for small cell data offloading in heterogeneous cellular network," *J. Commun.*, vol. 15, no. 1, pp. 1–13, 2020.

[5] S. C. Lam and K. Sandrasegaran, "Fractional frequency reuse in multi-tier networks: Performance analysis and optimization," *Int. J. Wirel. Inf. Networks*, vol. 27, no. 1, pp. 164–183, 2020.

[6] S. Chang, S. Kim, and J. P. Choi, "The optimal distance threshold for fractional frequency reuse in size-scalable

networks," *IEEE Trans. Aerosp. Electron. Syst.*, vol. 56, no. 1, pp. 527–546, Feb. 2020.

[7] S. A. Khan, A. Kavak, S. A. Çolak, and K. Küçük, "A novel fractional frequency reuse scheme for interference management in LTE-A HetNets," *IEEE Access*, vol. 7, pp. 109662–109672, 2019.

[8] N. Saquib, E. Hossain, and D. Kim, "Fractional frequency reuse for interference management in LTE-advanced hetnets," *IEEE Wirel. Commun.*, vol. 20, no. 2, pp. 113–122, Apr. 2013.

[9] J. Andrews, F. Baccelli, and R. Ganti, "A tractable approach to coverage and rate in cellular networks," *IEEE Trans. Commun.*, vol. 59, no. 11, pp. 3122–3134, 2011.

[10] J. G. Andrews, "Seven ways that HetNets are a cellular paradigm shift," *IEEE Commun. Magzine*, vol. 51, no. 3, pp. 136–144, Mar. 2013.

[11] D. G. González and M. G. Lozano, "On the performance of static inter-cell interference coordination in realistic cellular layouts," *Mob. Networks Manag. Springer*, vol. 02, pp. 163–176, 2011.

[12] G. Gonzalez, *et al.*, "Optimization of soft frequency reuse for irregular LTE macrocellular networks," *IEEE Trans. Wirel. Commun.*, vol. 12, no. 5, pp. 2410–2423, 2013.

[13] T. D. Novlan, *et al.*, "Analytical evaluation of fractional frequency reuse for OFDMA cellular networks," *IEEE Trans. Wirel. Commun.*, vol. 10, no. 12, pp. 4294–4305, 2011.

[14] T. Novlan and R. Ganti, "Analytical evaluation of fractional frequency reuse for heterogeneous cellular networks," *IEEE Transactions on Communications*, vol. 60, no. 7, pp. 2029–2039, 2012.

[15] S. C. Lam and Q. T. Nguyen, "A general model of fractional frequency reuse: modelling and performance analysis," *JVNU ournal Sci. Comput. Sci. Commun.*, vol. 36, no. 1, 2020.

[16] R. Ullah, N. Fisal, H. Safda, Z. Khalid, W. Maqbool, and H. Ullah, "Stochastic geometry based dynamic fractional frequency reuse for OFDMA systems," *J. Teknol. (Sciences Eng.*, vol. 67, no. 1, 2014.

[17] R. Ullah, N. Fisal, and H. Safdar, "Fractional frequency reuse for irregular cell geometry OFDMA systems," in *Proc. IEEE Int. Symp. Telecommun. Technol. (ISTT 2014)*, Langkawi, Malaysia, 2014.

[18] R. Ullah, N. Fisal, H. Safdar, Z. Khalid, and W. Maqbool, "Fractional frequency reuse for irregular geometry based heterogeneous cellular networks," in *Proc. 5th Natl. Symp. Inf. Technol. Towar. New Smart World*, 2015, pp. 5–10.

[19] H. ElSawy, E. Hossain, and M. Haenggi, "Stochastic geometry for modeling, analysis, and design of multi-tier and cognitive cellular wireless networks: A survey," *IEEE Commun. Surv. Tutorials*, vol. 15, no. 3, pp. 996–1019, 2013.

[20] A. Baert, D. Sem, D. Picardie, and J. Verne, "Voronoi mobile cellular networks : Topological properties," *Parallel Distrib. Comput. 2004. Third Int. Symp. on/Algorithms, Model. Tools Parallel Comput. Heterog. Networks, 2004. Third Int. Work.*, 2004.

[21] 3GPP, "3gpp tr 25.996 V10.0.0 (2011-03)," vol. 0, no. Release 10, 2011.

Dr. Rahat Ullah received his PhD degree in Electrical Engineering from Universiti Teknologi Malaysia (UTM) in 2016, MS degree in Electronic Engineering from International Islamic University Islamabad in 2010, and B.Sc Electrical Engineering degree from CECOS University of IT and Emerging Sciences, Peshawar in 2006. He is currently working as Head of Department and Assistant Professor at the Department of Electrical Engineering, FUUAST, Islamabad. His research interests include resource allocation and interference management in wireless cellular networks.

Dr. Hanif Ullah, senior member IEEE, received his Ph.D degree in Electrical Engineering from Universitat PoliTecnica de Valencia (UPV) Spain in 2015 and M.S degree in Electronic Engineering from International Islamic University Islamabad, Pakistan in 2011. He is currently Assistant Professor at the Department of Electrical Engineering, FUUAST, Islamabad. His research interests include Optical Communication, Optoelectronic devices, Renewable Energy Technologies, PHOTOVOLTAIC Solar Cells/Systems.

Dr. Zubair Khalid received his Ph.D. degree in Electrical Engineering from Universiti Teknologi Malaysia (UTM) Malaysia in 2017 and M.S in Electrical Engineering from University of Engineering and Technology, Taxila in 2012. He is currently Assistant Professor at the Department of Electrical Engineering, FUUAST, Islamabad. His research interests include IoT, WSN for smart home ambient assisted living, middleware design for virtual sensor networks.

Dr. Hashim Safdar received his PhD degree in Electrical Engineering from Universiti Teknologi Malaysia (UTM) in 2017 and MS degree in Electrical Engineering from Blekinge Institute of Technology, Sweden, in 2008. He is currently Assistant Professor at the Department of Electrical Engineering, FUUAST, Islamabad. His research interests include resource allocation and interference management in wireless cellular networks. His research interests include resource allocation in M2M and cellular communication.